

ISSN: 0256-307X

# 中国物理快报

# Chinese Physics Letters

Volume 32 Number 6 June 2015

A Series Journal of the Chinese Physical Society  
Distributed by IOP Publishing

Online: <http://iopscience.iop.org/0256-307X>  
<http://cpl.iphy.ac.cn>

CHINESE PHYSICAL SOCIETY  
**IOP** Publishing

JUST FOR AUTHORS  
— CHINESE PHYSICS LETTERS

## On the Fundamental Mode Love Wave in Devices Incorporating Thick Viscoelastic Layers \*

LIU Jian-Sheng(刘建生)\*\* , WANG Li-Jun(王立君), HE Shi-Tang(何世堂)

*Institute of Acoustics, Chinese Academy of Sciences, Beijing 100190*

(Received 5 February 2015)

A detailed investigation is presented for Love waves (LWs) with thick viscoelastic guiding layers. A theoretical calculation and an experiment are carried out for LW devices incorporating an SU-8 guiding layer, an ST-90° X quartz substrate and two 28- $\mu\text{m}$  periodic interdigital transducers. Both the calculated and the measured results show an increase in propagation velocity when  $h/\lambda > 0.05$ . The measured insertion loss of LWs is consistent with the calculated propagation loss. The insertion loss of bulk waves is also measured and is compared with that of LWs.

PACS: 43.35.+d, 43.38.+n, 62.20.-x

DOI: 10.1088/0256-307X/32/6/064301

Recently a growing number of acoustic wave modes<sup>[1–3]</sup> have been applied in various fields. Among the modes, Love wave (LW) sensors have been attracting much attention since they were used for bio (chemical) sensing applications.<sup>[4,5]</sup> The detector of an LW based sensor consists of a semi-infinite piezoelectric substrate which supports shear horizontal (SH) waves, a guiding layer in which the transverse acoustic wave is slower than that in the substrate, and interdigital transducers (IDTs) which are deposited on the substrate surface for exciting and receiving SH waves. The maximum sensitivity has been proved, occurring at the maximum slope of the dispersion curve. To achieve a higher sensitivity, LW devices have been reported<sup>[6,7]</sup> incorporating guiding layers consisting of polymeric materials which have slower transverse waves and lower density than the commonly used silicon dioxide. Due to the viscoelasticity of polymers, most developed LW devices incorporate guiding layers that are much thinner than the optimum thickness. Only McHale *et al.*<sup>[8]</sup> and Newton *et al.*<sup>[9]</sup> carried out experimental study on the resonant conditions and insertion loss changes of LW devices with thick S1813 photoresist layers on ST-cut quartz substrates. In their experiments, the first higher order mode LW was found, occurring at the relative layer thickness of  $h/\lambda = 0.06$ , which is much thinner than the theoretical thickness. To the best of our best knowledge, there is still no reasonable theoretical explanation for this abnormal phenomenon.

In this Letter, we present a detailed investigation on LW devices with thick viscoelastic guiding layers. A theoretical calculation is carried out for LW devices incorporating an SU-8 guiding layer, an ST-90° X quartz substrate and two 28- $\mu\text{m}$  periodic IDTs. The experimental devices are fabricated and measured. The calculated velocity agrees well with

the measured result and it shows that the guiding layer viscoelasticity causes an increase in the LWs propagation velocity. The insertion loss of LWs is measured, which is consistent with the calculated propagation loss. The insertion loss of bulk waves (BWs) is also measured and is compared with that of LWs. The results and discussions presented in this work will be helpful in analyzing and optimizing the performances of LW based sensors incorporating polymeric layers.

The substrate of an LW device must be a material which supports pure piezoelectric SH acoustic waves.<sup>[10,11]</sup> The most commonly used substrate is ST-cut quartz, which has a tiny piezoelectricity and an obvious anisotropy, thus it can be considered as an anisotropic medium. The guiding layer is an isotropic material which is coated on the substrate surface with a thickness of  $h$ . The dispersion equation<sup>[12]</sup> of LWs in such a structure is

$$\mu_L \beta_L \tan(\beta_L kh) = c_{44} \bar{\beta}_S, \quad (1)$$

where  $k = \omega/v$  is the propagation factor of LWs,  $\omega$  is the angular frequency,  $v$  is the propagation velocity,  $\beta_L = \sqrt{v^2/(V_L)^2 - 1}$  is the particle displacement distribution factor in the guiding layer,  $V_L = \sqrt{\mu_L/\rho_L}$  is the phase velocity of transverse acoustic waves in the layer,  $\mu_L$  and  $\rho_L$  are the shear modulus and density of the guiding layer, respectively,  $\bar{\beta}_S = \sqrt{(V_{S1}^2 - v^2)/V_{S2}^2}$  is the real part of the distribution factor in the substrate,  $V_{S1} = \sqrt{(c_{66} - c_{46}^2/c_{44})/\rho_S}$  is the velocity of quasi-SH waves propagating in the same direction to LWs,  $V_{S2} = \sqrt{c_{44}/\rho_S}$  is the velocity of SH-polarization and propagating in the vertical direction,  $c_{44}$ ,  $c_{46}$  and  $c_{66}$  are elastic constants of the substrate, and  $\rho_S$  is the density of the substrate.

Different from elastic overlays, a polymer guiding layer will produce a large propagation attenuation due

\*Supported by the National Natural Science Foundation of China under Grant No 11104314.

\*\*Corresponding author. Email: liujs98@hotmail.com

© 2015 Chinese Physical Society and IOP Publishing Ltd

to its non-ignorable viscosity. When the viscoelasticity is included, the shear modulus  $\mu_L$  of the guiding layer becomes a complex variant. The mechanical behavior of a viscoelastic material can be described by using the Maxwell–Weichert model<sup>[13]</sup> consisting of springs and dashpots. In this work, a simplified model incorporating an elastic branch and a Maxwell branch is adopted. Thus the complex shear modulus can be expressed as

$$\mu_L = \mu_0 + \mu_1 \frac{i\omega\tau_1}{1 + i\omega\tau_1}, \quad (2)$$

where  $\tau_1 = \eta_1/\mu_1$  is the relaxation time of the Maxwell branch,  $\mu_0$  and  $\mu_1$  are elastic constants of the elastic branch and the Maxwell branch respectively, and  $\eta_1$  is the viscosity of the Maxwell branch. Substituting the complex  $\mu_L$  into the dispersion equations, we can obtain a complex velocity  $v = v_r + iv_i$ . Here  $v_r$  represents the propagation velocity in the  $x_1$  direction, while  $v_i$  is related to the propagation loss in the  $x_1$  direction. The insertion loss (IL) reads

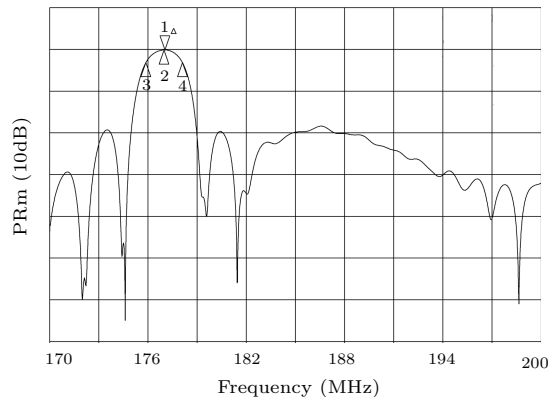
$$\text{IL} = 20 \log_{10} e^{\text{Im}(\omega/v)} \approx -54.6 \frac{v_i}{v_r}. \quad (3)$$

The LW devices used in our experiments consist of an ST-cut and 90° X-propagation quartz substrate with two lithographically defined Al (200 nm) IDTs. The IDTs are of aperture 2 mm and separated by a path length (center to center distance) of 4 mm. Each IDT consists of 72 periods of split-electrodes, with a wavelength of  $\lambda = 28 \mu\text{m}$  (3.5  $\mu\text{m}$  electrode widths and spacings).

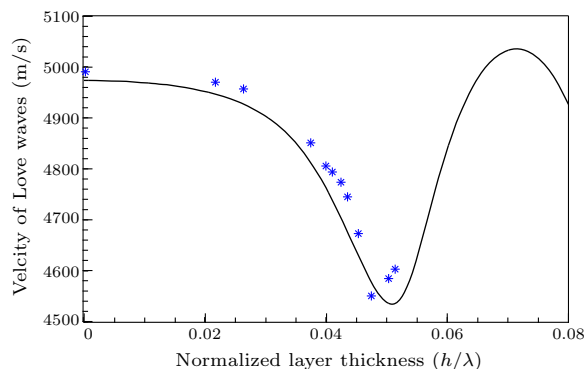
A guiding layer was deposited on the device surface by spin coating a solution of SU-8 2050 (with a volume ratio of 1:3 to the diluent agent), where a negative epoxy-based photoresist was obtained with MicroChem equipment. To achieve different layer thicknesses, we took the rotating speed ranging from 1000 to 5000 rpm and different spinning times, and the layer was post-cured by heating the device for 30 min at 150°C. The film on the wire pad was removed by using a sharp scalped blade. The thickness of the prepared SU-8 layer was measured by using an Alpha-step IQ surface profiler (KLA-Tencor, San Jose, CA). The coated wafer was divided into several LW devices. Then each device was mounted on a rectangular DIP header with electrical connections made by Al wires bonding. The input and output impedances of the Love device were matched to around 50  $\Omega$  by using LC circuits. Two SMA connectors were applied to connect the device and an HP8753D network analyzer.

Figure 1 shows the frequency response  $S_{21}$  of the LW device covered a 0.74- $\mu\text{m}$ -thick SU-8 guiding layer. There are two obvious signals. One is located at the frequency of 177.0 MHz (the corresponding propagation velocity of 4956.6 m/s), which is caused by the

fundamental mode of LWs. The insertion loss of LWs is of about 10 dB. Another signal is distributed between 182–191 MHz (the corresponding propagation velocity of 5096–5348 m/s), which is probably caused by bulk waves. The insertion loss of bulk waves is about 30 dB.



**Fig. 1.** Frequency response of the LW device coated with a 0.74- $\mu\text{m}$ -thick SU-8 layer.



**Fig. 2.** Theoretical and experimental velocities of the fundamental Love mode.

Figure 2 shows the calculated (solid line) and measured (stars) propagation velocities as a function of the normalized layer thickness ( $h/\lambda$ ). In the numerical calculations, the material parameters of the substrate (ST-90° X quartz)<sup>[12]</sup> are assumed: the elastic constants of  $c_{66} = 67.47 \text{ GPa}$ ,  $c_{44} = 30.34 \text{ GPa}$ ,  $c_{46} = -7.60 \text{ GPa}$ , and the density of  $\rho = 2651 \text{ kg/m}^3$ ; the parameters of the guiding layer (SU-8) are assumed:  $\mu_0 = 0.94 \text{ GPa}$ ,  $\mu_1 = 0.71 \text{ GPa}$ ,  $\tau_1 = 0.9 \text{ ns}$ , and  $\rho_L = 1215 \text{ kg/m}^3$ . As shown in Fig. 2, initially the propagation velocity is slowly reduced by increasing the guiding layer thickness. During the calculations, the substrate piezoelectricity is ignored, which will cause a reduction of  $\sim 20 \text{ m/s}$  in propagation velocity of the fundamental Love mode;<sup>[12]</sup> therefore the theoretical velocity is lower than the experimental values.

When  $h/\lambda$  exceeds 0.03, the velocity reducing is sped up, which is proved in an optimum region to achieve a large mass loading sensitivity. When  $h/\lambda$  exceeds 0.05, the reducing is decreased rapidly and

even a raising velocity is obtained as the layer is further thickened. The theoretical velocity can reach up to 5050 m/s at  $h/\lambda = 0.07$ , which is equivalent to the velocity of SSBW in the substrate. This result coincides with some previously reported experimental results.<sup>[8,14]</sup>

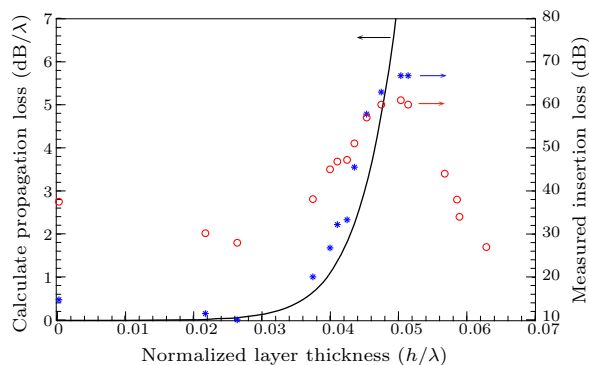


**Fig. 3.** Theoretical propagation loss (solid line) of the fundamental Love mode and measured insertion loss of LWs (asterisks) and BWs (circles).

For a Love device, the insertion loss is decided by IDT structures, the electromechanical coupling factor and the propagation loss, which is caused by the viscosities of the guiding layer and the substrate. In this work, the substrate is considered as an elastic material, thus the propagation loss is mainly caused by the polymeric guiding layer. Figure 3 shows the calculated propagation loss (solid line) of the fundamental Love mode, the measured insertion loss of LWs (asterisks) and bulk waves (circles). As the guiding layer is thickened, the calculated propagation loss is always being increased. When  $h/\lambda < 0.03$ , the propagation loss is relatively small and increased very slowly; thus the device insertion loss is mainly decided by the electromechanical coupling factor rather than the propagation loss. As mentioned in previous reports, the electromechanical coupling factor is initially increased with thickening the guiding layer and is seldom affected by the viscosities of guiding layers. Therefore, the measured device insertion loss is decreased with thickening the guiding layer. When  $h/\lambda > 0.03$ , the propagation loss is increased at an increasing speed with thickening the guiding layer; the attenuated acoustical energy caused by increasing propagation loss exceeds the increased energy produced by enlarging the electromechanical coupling factor. Therefore, the insertion loss of LWs is increased when the guiding layer is further thickened. As  $h/\lambda > 0.05$ , the propagation loss is increased at an accelerating rate while the electromechanical coupling factor starts to be decreased, thus

the device insertion loss is increased very rapidly and soon the signal of LWs is too weak to be detected.

The insertion loss of bulk waves is shown by circles in Fig. 3. When  $h/\lambda < 0.05$ , the insertion loss of bulk waves is also first decreased and then increased, which is similar to that of LWs. When  $h/\lambda > 0.05$ , the insertion loss is quickly increased with thickening the guiding layer. It should be noted that when  $h/\lambda > 0.043$ , the insertion loss of bulk waves is less than that of LWs. This phenomenon is easily misunderstood as the start of the first higher order Love mode. In fact, the theoretical starting layer thickness<sup>[15]</sup> is  $h = \frac{\lambda}{2\sqrt{V_s^2/V_L^2 - 1}} \approx \frac{\lambda}{9}$ .

In conclusion, we have shown a detailed investigation on LW devices incorporating a thick viscoelastic guiding layer. When the relative guiding layer exceeds 0.05, the theoretical result shows that the viscoelasticity causes an increase in the propagation velocity of LWs, and the result is confirmed with the experimental devices. The insertion losses of LWs and bulk waves are also measured and analyzed. The calculated propagation loss is consistent with the measured insertion loss of LWs. The results and discussions presented in this work will be helpful in analyzing and optimizing the performances of LW based sensors incorporating polymeric layers.

## References

- [1] Kim C and Jhang K 2012 *Chin. Phys. Lett.* **29** 120701
- [2] Khaled S M, Soliman R K and Sara I A 2013 *Chin. Phys. B* **22** 124702
- [3] Tan F and Huang X 2013 *Chin. Phys. Lett.* **30** 050701
- [4] Gizeli E, Stevenson A C, Goddard N J and Lowe C R 1992 *IEEE Trans. Ultrason. Ferroelectr. Freq. Contr.* **39** 657
- [5] Kovacs G, Lubking G W, Vellekoop M J and Venema A 1992 *IEEE Ultrason. Symp. Proc.* (Tucson Arizona, USA 20–23 October 1992) p 281
- [6] McHale G, Newton M I and Martin F 2003 *J. Appl. Phys.* **93** 675
- [7] Matatagui D, Fernández M J, Fontecha J, Sayago I, Gràcia I, Cané C, Horrillo M C and Santos J P 2014 *Talanta* **120** 408
- [8] McHale G, Newton M I, Martin F, Gizeli E and Melzak K A 2001 *Appl. Phys. Lett.* **79** 3542
- [9] Newton M I, McHale G and Martin F 2004 *Sens. Actuators A* **109** 180
- [10] Jakoby B and Vellekoop M J 1997 *Smart Mater. Struct.* **6** 668
- [11] Liu J and He S 2010 *Int. J. Solids Struct.* **47** 169
- [12] Liu J 2014 *AIP Adv.* **4** 077102
- [13] Liu J, Wang L, Lu Y and He S 2013 *Smart Mater. Struct.* **22** 125034
- [14] Penza M and Cassano G 2000 *Sens. Actuators B* **68** 300
- [15] Zimmermann C, Rebière D, Déjous C, Pistré J, Chastaing E and Planade R 2001 *Sens. Actuators B* **76** 86

# Chinese Physics Letters

Volume 32

Number 6

June 2015

## GENERAL

- 060301 Critical Behavior of the Energy Gap and Its Relation with the Berry Phase Close to the Excited State Quantum Phase Transition in the Lipkin Model**  
YUAN Zi-Gang, ZHANG Ping
- 060302 Robustness of Genuine Tripartite Entanglement under Collective Dephasing**  
MAZHAR Ali
- 060303 Quantum State Transfer among Three Ring-Connected Atoms**  
GUO Yan-Qing, DENG Yao, PEI Pei, TONG Dian-Min, WANG Dian-Fu, MI Dong
- 060304 The Coherence of a Dipolar Condensate in a Harmonic Potential Superimposed to a Deep Lattice**  
WANG Long, YU Zi-Fa, XUE Ju-Kui
- 060501 The Effect of Quantum Coins on the Spreading of Binary Disordered Quantum Walk**  
ZHAO Jing, HU Ya-Yun, TONG Pei-Qing
- 060502 The Dependence of Chimera States on Initial Conditions**  
FENG Yue-E, LI Hai-Hong

## NUCLEAR PHYSICS

- 062101 Description of the Shape Coexistence in  $^{98}\text{Mo}$  with IBM2**  
ZHANG Da-Li, YUAN Shu-Qing, DING Bin-Gang,
- 062501 Azimuthal Asymmetry of Pion-Meson Emission around the Projectile and Target Sides in Au+Au Collision at 1A GeV**  
WANG Ting-Ting, L Ming, MA Yu-Gang, FANG De-Qing, WANG Shan-Shan, ZHANG Guo-Qiang

## ATOMIC AND MOLECULAR PHYSICS

- 063101 A High-Precision Calculation of Bond Length and Spectroscopic Constants of  $\text{Hg}_2$  Based on the Coupled-Cluster Theory with Spin-Orbit Coupling**  
TU Zhe-Yan, WANG Wen-Liang
- 063201 Population Distribution of Excited States in Cs Electrodeless Discharge Lamp**  
ZHU Chuan-Wen, TAO Zhi-Ming, CHEN Mo, LIU Zhong-Zheng, ZHANG Xiao-Gang, ZHANG Sheng-Nan, CHEN Jing-Biao
- 063301 Charge Resonance Enhanced Multiple Ionization of  $\text{H}_2\text{O}$  Molecules in Intense Laser Fields**  
LIU Hong, LI Min, XIE Xi-Guo, WU Cong, DENG Yong-Kai, WU Cheng-Yin, GONG Qi-Huang, LIU Yun-Quan
- 063302 Generation of Isolated Attosecond Pulse from Asymmetric Molecular Ions by Introducing Half-Cycle-Like Laser Fields**  
LIU Sha-Sha, MIAO Xiang-Yang
- 063303 Photon Statistical Properties of Single Terrylene Molecules in P-Terphenyl Crystals**  
HAN Bai-Ping, ZHENG Yu-Jun, HU Feng, FAN Qiu-Bo

## FUNDAMENTAL AREAS OF PHENOMENOLOGY (INCLUDING APPLICATIONS)

- 064201 A kW Continuous-Wave Ytterbium-Doped All-Fiber Laser Oscillator with Domestic Fiber Components and Gain Fiber**  
LIAO Lei, LIU Peng, XING Ying-Bin, WANG Yi-Bo, PENG Jing-Gang, DAI Neng-Li, LI Jin-Yan, HE Bing, ZHOU Jun
- 064202 Probing of Ultrafast Plasmon Dynamics on Gold Bowtie Nanostructure Using Photoemission Electron Microscopy**  
QIN Jiang, JI Bo-Yu, HAO Zuo-Qiang, LIN Jing-Quan

JUST FOR AUTHORS  
— CHINESE PHYSICS LETTERS

- 064203 Optimization of High Power 1.55- $\mu\text{m}$  Single Lateral Mode Fabry–Perot Ridge Waveguide Lasers**  
KE Qing, TAN Shao-Yang, LU Dan, ZHANG Rui-Kang, WANG Wei, JI Chen
- 064204 Propagation of Partially Coherent Elegant Hermite-Cosh-Gaussian Beam in Non-Kolmogorov Turbulence**  
ZHANG Wen-Fu, LIAN Jie, WANG Ying-Shun, HU Xue-Yuan, SUN Zhao-Zong, ZHAO Ming-Lin, WANG Ying, LI Meng-Meng
- 064205 Simultaneously Suppressing Low-Frequency and Relaxation Oscillation Intensity Noise in a DBR Single-Frequency Phosphate Fiber Laser**  
XIAO Yu, LI Can, XU Shan-Hui, FENG Zhou-Ming, YANG Chang-Sheng, ZHAO Qi-Lai, YANG Zhong-Min
- 064206 Extraordinary Optical Confinement in a Silicon Slot Waveguide with Metallic Gratings**  
LIANG Han, ZHAN Ke-Tao, HOU Zhi-Ling
- 064207 Effect of In Diffusion on the Property of Blue Light-Emitting Diodes**  
ZENG Yong-Ping, LIU Wen-Jie, WENG Guo-En, ZHAO Wan-Ru, ZUO Hai-Jie, YU Jian, ZHANG Jiang-Yong, YING Lei-Ying, ZHANG Bao-Ping
- 064208 In-Fiber Mach–Zehnder Interferometer Based on Waist-Enlarged Taper and Core-Mismatching for Strain Sensing**  
ZHANG Yun-Shan, QIAO Xue-Guang, SHAO Min, LIU Qin-Peng
- 064209 Stable Q-Switched Yb:NaY(WO<sub>4</sub>)<sub>2</sub> Laser with Cr<sup>4+</sup>:YAG Saturable Absorber**  
LAN Rui-Jun
- 064210 Transverse Optical Properties of the Eu<sup>3+</sup>:Y<sub>2</sub>SiO<sub>5</sub> Crystal in Electromagnetically Induced Transparency**  
YANG Li-Ru, WANG Chun-Fang, ZHANG Da-Wei
- 064211 Cold Atom Cloud with High Optical Depth Measured with Large Duty Cycle**  
ZHANG Jun, GU Zhen-Jie, QIAN Peng, HAN Zhi-Guang, CHEN Jie-Fei
- 064301 On the Fundamental Mode Love Wave in Devices Incorporating Thick Viscoelastic Layers**  
LIU Jian-Sheng, WANG Li-Jun, HE Shi-Tang
- 064302 The Effects of Seamounts on Sound Propagation in Deep Water**  
LI Wen, LI Zheng-Lin, ZHANG Ren-He, QIN Ji-Xing, LI Jun, NAN Ming-Xing
- 064303 Horizontal-Longitudinal Correlations of Acoustic Field in Deep Water**  
LI Jun, LI Zheng-Lin, REN Yun, LI Wen, ZHANG Ren-He

## PHYSICS OF GASES, PLASMAS, AND ELECTRIC DISCHARGES

- 065201 Electron Cyclotron Emission Imaging Observations of  $m/n = 1/1$  and Higher Harmonic Modes during Sawtooth Oscillation in ICRF Heating Plasma on EAST**  
AZAM Hussain, GAO Bing-Xi, LIU Wan-Dong, XIE Jin-Lin, the EAST Team
- 065202 Negative Refraction in a Lossy Plasma Layer**  
PENG Li, GUO Bin, GAO Ming-Xiang, CAI Xin
- 065203 Simulation of Plasma Disruptions for HL-2M with the DINA Code**  
XUE Lei, DUAN Xu-Ru, ZHENG Guo-Yao, LIU Yue-Qiang, YAN Shi-Lei, DOKUKA V. V., KHAYRUTDINOV R. R., LUKASH V. E.

## CONDENSED MATTER: STRUCTURE, MECHANICAL AND THERMAL PROPERTIES

- 066101 Enhanced Magnetic and Dielectric Properties in Low-Content Tb-Doped BiFeO<sub>3</sub> Nanoparticles**  
GUO Min-Chen, LIU Wei-Fang, WU Ping, ZHANG Hong, XU Xun-Ling, WANG Shou-Yu, RAO Guang-Hui

JUST FOR AUTHORS  
— CHINESE PHYSICS LETTERS

## CONDENSED MATTER: ELECTRONIC STRUCTURE, ELECTRICAL, MAGNETIC, AND OPTICAL PROPERTIES

- 067301 Bismuth Effects on Electronic Levels in GaSb(Bi)/AlGaSb Quantum Wells Probed by Infrared Photoreflectance**  
CHEN Xi-Ren, SONG Yu-Xin, ZHU Liang-Qing, QI Zhen, ZHU Liang, ZHA Fang-Xing, GUO Shao-Ling, WANG Shu-Min, SHAO Jun
- 067302 First-Principles Calculations of the Quantum Size Effects on the Stability and Reactivity of Ultrathin Ru(0001) Films**  
WU Ming-Yi, JIA Yu, SUN Qiang
- 067303 Identification of Topological Surface State in PdTe<sub>2</sub> Superconductor by Angle-Resolved Photoemission Spectroscopy**  
LIU Yan, ZHAO Jian-Zhou, YU Li, LIN Cheng-Tian, LIANG Ai-Ji, HU Cheng, DING Ying, XU Yu, HE Shao-Long, ZHAO Lin, LIU Guo-Dong, DONG Xiao-Li, ZHANG Jun, CHEN Chuang-Tian, XU Zu-Yan, WENG Hong-Ming, DAI Xi, FANG Zhong, ZHOU Xing-Jiang
- 067401 Electronic Structure, Irreversibility Line and Magnetoresistance of Cu<sub>0.3</sub>Bi<sub>2</sub>Se<sub>3</sub> Superconductor**  
YI He-Mian, CHEN Chao-Yu, SUN Xuan, XIE Zhuo-Jin, FENG Ya, LIANG Ai-Ji, PENG Ying-Ying, HE Shao-Long, ZHAO Lin, LIU Guo-Dong, DONG Xiao-Li, ZHANG Jun, CHEN Chuang-Tian, XU Zu-Yan, GU Gen-Da, ZHOU Xing-Jiang
- 067402 Possible p-Wave Superconductivity in Epitaxial Bi/Ni Bilayers**  
GONG Xin-Xin, ZHOU He-Xin, XU Peng-Chao, YUE Di, ZHU Kai, JIN Xiao-Feng, TIAN He, ZHAO Ge-Jian, CHEN Ting-Yong
- 067501 Evaluation of the Ultrafast Thermal Manipulation of Magnetization Precession in Ferromagnetic Semiconductor (Ga,Mn)As**  
LI Hang, ZHANG Xin-Hui
- 067502 Magnetization Reversal Process of Single Crystal  $\alpha$ -Fe Containing a Nonmagnetic Particle**  
LI Yi, XU Ben, HU Shen-Yang, LI Yu-Lan, LI Qiu-Lin, LIU Wei
- 067503 Nitrogen-Induced Change of Magnetic Properties in Antiperovskite-Type Carbide: Mn<sub>3</sub>InC**  
MALIK Muhammad-Imran, SUN Ying, DENG Si-Hao, SHI Ke-Wen, HU Peng-Wei, WANG Cong
- 067601 Magnetic Field Measurement with Heisenberg Limit Based on Solid Spin NOON State**  
ZHOU Lei-Ming, DONG Yang, SUN Fang-Wen

## CROSS-DISCIPLINARY PHYSICS AND RELATED AREAS OF SCIENCE AND TECHNOLOGY

- 068101 Graphene-Based Tunable Polarization Insensitive Dual-Band Metamaterial Absorber at Mid-Infrared Frequencies**  
ZHANG Yu-Ping, LI Tong-Tong, LV Huan-Huan, HUANG Xiao-Yan, ZHANG Xiao, XU Shi-Lin, ZHANG Hui-Yun
- 068102 Theoretical and Experimental Optimization of InGaAs Channels in GaAs PHEMT Structure**  
GAO Han-Chao, YIN Zhi-Jun
- 068103 Simulation of Dendritic Growth with Melt Convection in Solidification of Ternary Alloys**  
SUN Dong-Ke, ZHANG Qing-Yu, CAO Wei-Sheng, ZHU Ming-Fang
- 068104 Molecular Beam Epitaxy Growth and Scanning Tunneling Microscopy Study of Pyrite CuSe<sub>2</sub> Films on SrTiO<sub>3</sub>**  
PENG Jun-Ping, ZHANG Hui-Min, SONG Can-Li, JIANG Ye-Ping, WANG Li-Li, HE Ke, XUE Qi-Kun, MA Xu-Cun
- 068301 Set Programming Method and Performance Improvement of Phase Change Random Access Memory Arrays**  
FAN Xi, CHEN Hou-Peng, WANG Qian, WANG Yue-Qing, LV Shi-Long, LIU Yan, SONG Zhi-Tang, FENG Gao-Ming, LIU Bo
- 068501 Ultralow Specific on-Resistance Trench MOSFET with a U-Shaped Extended Gate**  
WANG Zhuo, LI Peng-Cheng, ZHANG Bo, FAN Yuan-Hang, XU Qing, LUO Xiao-Rong

**068502 The Cu Based AlGa<sub>N</sub>/Ga<sub>N</sub> Schottky Barrier Diode**

LI Di, JIA Li-Fang, FAN Zhong-Chao, CHENG Zhe, WANG Xiao-Dong, YANG Fu-Hua, HE Zhi

**068503 A Strategy for Magnifying Vibration in High-Energy Orbits of a Bistable Oscillator at Low Excitation Levels**

WANG Guang-Qing, LIAO Wei-Hsin

**068701 Dynamics of Nano-Chain Diffusing in Porous Media**

CHEN Jiang-Xing, ZHENG Qiang, HUANG Chun-Yun, XU Jiang-Rong, YING He-Ping

**068901 Structural Modeling and Characteristics Analysis of Flow Interaction Networks in the Internet**

WU Xiao-Yu, GU Ren-Tao, PAN Zhuo-Ya, JIN Wei-Qi, JI Yue-Feng

**ERRATA AND OTHER CORRECTIONS**

**069901 Erratum: Laser-Induced Graphite Plasma Kinetic Spectroscopy under Different Ambient Pressures [Chin. Phys. Lett. Vol. 32, No. 4, 043201(2015)]**

K. Chaudhary, S. Rosalan, M. S. Aziz, M. Bahadoran, J. Ali, P. P. Yupapin, N. Bidin, Saktioto

**JUST FOR AUTHORS**  
— CHINESE PHYSICS LETTERS